

1 **The calibration and deployment of a low-cost methane sensor**

2 Stuart N. Riddick^{1,a}, Denise L. Mauzerall^{1,2}, Michael Celia¹, Grant Allen³, Joseph Pitt^{3,b}, Mary
3 Kang⁴ and John C. Riddick¹

4 ¹ Department of Civil and Environmental Engineering, Princeton University, Princeton, NJ 08544,
5 USA

6 ² Woodrow Wilson School of Public and International Affairs, Princeton University, Princeton,
7 NJ 08544, USA

8 ³ Centre for Atmospheric Science, University of Manchester, Manchester, M13 9PL, UK

9 ⁴ Department of Civil Engineering and Applied Mechanics, McGill University, Montreal, H3A
10 0C3, Canada

11 ^a now at The Energy Institute, Colorado State University, Fort Collins, CO 80523, USA

12 ^b now at School of Marine and Atmospheric Sciences, Stony Brook University, Stony Brook, NY
13 11794, USA

14 **Correspondence**

15 Stuart N. Riddick (Stuart.Riddick@colostate.edu) and Denise L. Mauzerall
16 (mauzeral@princeton.edu)

17 **Key Words**

18 Methane; mixing ratio; measurement; inexpensive; calibration

19 **Abstract**

20 Since 1850 the atmospheric mixing ratio of methane (CH₄), a potent greenhouse gas, has doubled.
21 This increase is directly linked to an escalation in emissions from anthropogenic sources. An
22 inexpensive means to identify and monitor CH₄ emission sources and evaluate the efficacy of
23 mitigation strategies is essential. However, sourcing reliable, low-cost, easy-to-calibrate sensors
24 that are fit for purpose is challenging. A recent study showed that CH₄ mixing ratio data from a
25 low-power, low-cost CH₄ sensor (Figaro TGS2600) agreed well with CH₄ mixing ratios measured
26 by a high precision sensor at mixing ratios between 1.85 ppm and 2 ppm. To investigate, as a
27 proof of concept, if this low-cost sensor could be used to measure typical ambient CH₄ mixing
28 ratios, we operated a TGS2600 in conjunction with a Los Gatos Ultra-portable Greenhouse Gas
29 Analyzer (UGGA) in controlled laboratory conditions. We then explored the sensor's long-term
30 reliability by deploying the TGS2600 near an onshore gas terminal to calculate emissions from
31 May to July 2018. Our initial studies showed that previously published linear algorithms could
32 not convert TGS2600 output to CH₄ mixing ratios measured by the UGGA. However, we derived
33 a non-linear empirical relationship that could be used to reliably convert the output of a TGS2600
34 unit to CH₄ mixing ratios over a range of 1.85 to 5.85 ppm that agree to a high-precision instrument
35 output to ± 0.01 ppm. Our study showed that the TGS2600 could be used to continuously measure
36 variability in CH₄ mixing ratios from 1.82 to 5.40 ppm for three months downwind of the gas
37 terminal. Using a simplified Gaussian Plume approach, these mixing ratios correspond to an
38 emission flux range of 0 to 238 g CH₄ s⁻¹, with average emission of 9.6 g CH₄ s⁻¹ from the currently
39 active North Terminal and 1.6 g CH₄ s⁻¹ from the decommissioned South Terminal. Our work
40 here demonstrates the feasibility of utilizing a low-cost sensor to detect methane leakage at
41 concentrations close to ambient background levels, as long as the device is routinely calibrated

42 with an accurate reference instrument. Having a widely deployed network of such low-cost CH₄
43 sensors would allow improved identification, monitoring and mitigation of a variety of CH₄
44 emissions.

45 **1 Introduction**

46 Methane (CH₄) is a greenhouse gas that is also partially responsible for production and loss of
47 tropospheric ozone. Since 1850 atmospheric CH₄ mixing ratios have increased from 715 ppb to
48 1865 ppb in 2005 (NOAA, 2019). This increase in mixing ratio is largely attributed to increased
49 anthropogenic emissions (Turner et al., 2019). The ability to estimate the size and location of CH₄
50 emissions is essential for all mitigation strategies and associated policies (de Coninck et al., 2018).
51 Current greenhouse gas emission inventories are principally compiled using industry-standard or
52 recommended emission factors, which are based on measurements made at a limited number of
53 sites, combined with estimates of activity levels (BEIS, 2018). Despite their widespread use,
54 recent studies suggest that the use of emission factors may be insufficient to describe CH₄
55 emissions from complex processes and direct measurements are preferable (Cerri et al., 2017;
56 Riddick et al., 2019b, 2019a; Turner et al., 2015; Yang et al., 2017). Emission estimates from
57 direct measurements are generally calculated using gas mixing ratios measured downwind of the
58 source.

59 For CH₄, current options for measuring near-ambient mixing ratios include spectroscopic
60 instruments, such as the Los Gatos UGGA or Picarro G2301 CRDS instruments which cost
61 between \$50,000 and \$100,000 each, or lower cost gas chromatographs costing around \$10,000
62 each. These instruments are high precision (1 standard deviation < 2 ppb at 1 Hz) and have been
63 used on long-term measurements campaigns for autonomous measurements (Connors et al., 2018;
64 Riddick et al., 2018, 2017). However, power consumption demands (~260 W) mean they require
65 a continuous electricity supply for deployment longer than an hour at most and insurance
66 requirements for these expensive instruments demand locked and secure premises, which means
67 that many remote locations cannot be measured.

68 Various government and industry/non-profit initiatives, such as the U.S. Department of Energy's
69 MONITOR program and the Environmental Defense Fund's Methane Detector Challenge, support
70 the research and development of new technologies to measure CH₄ mixing ratios. These methods
71 range from satellite-based methods to new laser-based methods. However, current systems cost
72 between \$10,000 and \$20,000 and the security of the instruments during measurement campaigns
73 remain an issue. Due to the importance of CH₄ emission reduction strategies (IPCC, 2018), testing
74 and deployment of low-cost CH₄ measurement devices is needed. This study investigates the use
75 of very low-cost sensors (~\$10) as an alternative to high-cost, high-precision instruments.

76 One example of a low power (~0.5 W), very low-cost sensor (~\$10 US dollars) is the Taguchi Gas
77 Sensor TGS2600 (Figaro Engineering Inc., Osaka, Japan) that is designed to measure ambient CH₄
78 mixing ratios between 1 and 100 ppm (Figaro, 2005). In 2012, Eugster and Kling (2012) reported
79 that CH₄ mixing ratios calculated from output of a TGS2600 at Toolik Lake, Alaska, USA were in
80 good agreement ($R^2 = 0.85$) with CH₄ mixing ratios measured by a Los Gatos Research FMA 100
81 CH₄ analyzer. However, the range of CH₄ mixing ratios reported by Eugster and Kling (2012)
82 was small, between between 1.85 and 2 ppm, relative to mixing ratios observed near active sources
83 of CH₄.

84 In this study, we report the findings of a measurement campaign to investigate the use of a
85 TGS2600 low-cost CH₄ sensor as an alternative to a high-cost, high-precision instrument. Our

86 goal is to assess the potential of deploying such sensors in large networks to identify a variety of
 87 methane leakage sources in order to improve greenhouse gas emission inventories. Our objectives
 88 are to: 1) Investigate if a TGS2600 sensor output can be used to estimate realistically observed
 89 CH₄ mixing ratio measurements of between 2 and 10 ppm; 2) Make long term measurements of
 90 CH₄ mixing ratios downwind of a natural gas point source using a TGS2600 without a mains power
 91 source or security measures; and 3) Estimate the emissions from a gas terminal using measured
 92 ambient methane mixing ratios and meteorological data. To our knowledge this is the first time
 93 that the low-cost TGS2600 sensor has been calibrated to quantify mixing ratios between 1.8 and
 94 5.8 ppm and then used to calculate fugitive CH₄ emissions from a natural gas point-source.

95 **2 Methods**

96 **2.1 Calculating methane mixing ratios from the TGS2600 output**

97 The TGS2600 is a solid-state sensor that uses titanium dioxide (TiO₂) as the sensing material.
 98 When the TiO₂ is heated, gases in the air adsorb to its surface and as the concentration of CH₄ in
 99 air increases the resistance of TiO₂ decreases (Figaro, 2005). The schematic diagram showing the
 100 setup of the TGS2600 in this application can be found on the TGS2600 datasheet (Figaro, 2005)
 101 and in Figure 2 in Eugster and Kling (2012). The TiO₂ has a resistance in clean air (R_0, Ω), i.e. air
 102 with ambient methane, which becomes lower in the presence of methane (R_s, Ω) and the ratio of
 103 these resistances (R_s/R_0) gives a measure of the CH₄ mixing ratio in air. However, the resistance
 104 of TiO₂ is also affected by the air temperature ($T_a, ^\circ\text{C}$) and relative humidity ($rH, \%$) and the ratio
 105 of resistance must be corrected for these factors (Eq. 1). The uncalibrated CH₄ mixing ratio
 106 ($[CH_4]_{raw}$, ppm) can be calculated as a linear function of the corrected ratio of these resistances
 107 ($(R_s/R_0)_{corr}$) following the equation of Eugster and Kling (2012) (Eq. 2).

$$108 \quad \left(\frac{R_s}{R_0}\right)_{corr} = \left(\frac{R_s}{R_0} \cdot (0.024 + 0.0072 \cdot rH + 0.0246 \cdot T_a)\right) \quad (1)$$

$$109 \quad [CH_4]_{raw} = 1.8280 + 0.0288 \cdot \left(\frac{R_s}{R_0}\right)_{corr} \quad (2)$$

110 **2.3 Calibrating the TGS2600**

111 As Eugster and Kling (2012) reported, the TGS2600 does not measure CH₄ well in low relative
 112 humidity, i.e. < 40 %. Because of this, we could not easily calibrate the TGS2600 against cylinder
 113 reference standard gases of known (certified) concentrations, as these standards are typically very
 114 dry (often only a few ppm H₂O). As an alternative, we calibrated the TGS2600 by running it
 115 alongside a Los Gatos Research (Mountain View, CA, USA) Ultra-portable Greenhouse Gas
 116 Analyzer (UGGA). We conducted three side-by-side experiments: 1. 21st to 22nd April 2018 in an
 117 indoor laboratory at the University of Manchester, UK; 2. 24th June at St Michael's Church,
 118 Rampside, UK and; 3. Between the 24th August and 3rd September 2018 at University of
 119 Manchester's measurement site at Plumpton Hall Farm, Lancashire, UK. In addition to side-by-
 120 side measurements with the UGGA, a second TGS2600 was run on the 3rd September 2018 to test
 121 for differences in output between sensors from the same manufacturer.

122 Using Equations 1 and 2, we calculated CH₄ mixing ratios using TGS2600 voltage output,
 123 temperature, and relative humidity data. Equation 2, the algorithm for calculating $[CH_4]_{raw}$, was
 124 then tuned for optimum performance using the UGGA CH₄ mixing ratio data as a reference. The
 125 metrics for selecting the most appropriate algorithm are the gradient and R² of the mixing ratios
 126 compared to the UGGA mixing ratios and the area under the mixing ratio time series. The area

127 under the mixing ratio time series is used as a measure of mass inferred by the measurements and
128 thought to be the best metric for choosing the most appropriate algorithm because it is expected
129 that the because of the passive nature of the TGS2600 it may not to respond to changes in mixing
130 ratio exactly at the same time as the UGGA, which has air pumped through the measurement
131 cavity.

132 **2.3 Case study – Measuring CH₄ emissions from a natural gas terminal**

133 **2.3.1 Methane emission source**

134 The Rampside gas terminal in Barrow-in-Furness, UK was chosen as the test site for the TGS2600
135 which was set up 1.5 km downwind at St. Michael’s church. This site was chosen because of its
136 accessibility and the relatively low emissions from the gas terminal, which provided a good test of
137 the detection ability of the TGS2600. The Rampside gas terminal collects and processes natural
138 gas from platforms in Morecambe Bay (Figure 1). It has two terminals - the North Terminal and
139 the South Terminal. In 2016 the South Terminal was decommissioned and all gas produced in
140 South Morecambe Bay was re-routed to the North Terminal. Spirit Energy, which operates the
141 terminal, expected that in 2018 the North Terminal would operate more efficiently than in previous
142 years and closer to design capacity, while the shuttered South Terminal would be expected to have
143 zero emissions (R. Davidson, Spirit Energy, pers. comm.).

144 Air from the North Terminal arrives at St Michael’s church when the wind blows from between
145 270 and 315°. During May, June and July 2018, when our measurements were made, the
146 Morcambe Bay platforms collectively produced an average of 0.49 Gg CH₄⁻¹ day⁻¹(OGA, 2018).
147 The latest CH₄ emission estimate published for the terminal was 0.68 Gg yr⁻¹, or 0.4 % of annual
148 production, in 2015, with the largest source of emissions associated with natural gas processing
149 (DEFRA, 2019). To put the emissions from this site in context, a landfill of area 0.1 km² emits 2
150 Gg CH₄ yr⁻¹(Riddick et al., 2017), while in 2017 larger UK gas terminals, Bacton and Easington,
151 emitted 1.6 and 1.0 Gg CH₄ yr⁻¹, respectively (BEIS, 2018).



152

153 *Figure 1 Location of the North and South Terminals at the Rampside gas terminal site in relation to the measurement location at*
 154 *St Michael's Church, Rampside. Images courtesy of Google Maps.*

155 **2.3.2 Deployment of TGS2600**

156 In this application, the TGS2600 was configured to give a DC voltage output corresponding to
 157 CH₄ mixing ratios of between 1 and 10 ppm. Sampling was controlled by an Arduino Uno
 158 microcomputer (Arduino, Ivrea, Italy), which digitizes and logs the voltage output from the sensor,
 159 and records the date and time, temperature, and relative humidity to a SD card at 1 minute intervals.
 160 The sensor was installed in the grounds of St Michael's Church, Rampside on 4th May 2018 (Figure
 161 1) and was powered by a 35 Ah lead acid battery which had sufficient capacity to operate the
 162 sampling and logging hardware for 7 days. The site was chosen because of proximity to the gas
 163 terminal, low background mixing ratios, and ease of access.

164 **2.3.3 Meteorological data**

165 Meteorological data were also collected at St Michael's Church, Rampside using a wireless
 166 weather station (Maplin, UK) attached to a mast 200 m from the nearest building and 2 m above
 167 the ground. The weather station was position 10 m away from the gas sensor and the location was
 168 chosen to jointly ensure an obstruction free wind field and security. Meteorological data were
 169 sampled and recorded at one-minute intervals and included: wind speed (u , m s⁻¹), wind direction
 170 (WD , ° to North), air temperature (T_a , K), relative humidity (RH , %), rain rate (R , mm hr⁻¹),
 171 irradiance (I , W m⁻²) and air pressure (P , Pa).

172 **2.3.4 Gaussian Plume Model**

173 A Gaussian plume (GP) model was used to calculate the emissions from the gas terminal. A GP
 174 model describes the mixing ratio of a gas as a function of distance downwind from a point source
 175 (Seinfeld and Pandis, 2016). As a gas is emitted, it is entrained in the prevailing ambient air flow
 176 and disperses in the y and z directions (relative to a mean horizontal flow in the x direction) with
 177 time, forming a dispersed concentration cone. The concentration of the gas (X , μg m⁻³), at any point

178 x metres downwind of the source, y metres laterally from the centre line of the plume and z metres
 179 above ground level can be calculated (Eq. 3) using the source strength (Q , g s^{-1}), the height of the
 180 source (h_s , m) and the Pasquill-Gifford stability class (PGSC) as a measure of air stability. The
 181 standard deviation of the lateral (σ_y , m) and vertical (σ_z , m) mixing ratio distributions are calculated
 182 from the Pasquill-Gifford stability class (PGSC) of the air (Pasquill, 1962; Busse and Zimmerman,
 183 1973; US EPA, 1995). The GP model assumes that the vertical eddy diffusivity and wind speed
 184 are constant and there is total reflection of CH_4 at the surface.

$$185 \quad X(x, y, z) = \frac{Q}{2\pi u \sigma_y \sigma_z} e^{-\frac{y^2}{(2\sigma_y)^2}} \left(e^{-\frac{(z-h_s)^2}{(2\sigma_z)^2}} + e^{-\frac{(z+h_s)^2}{(2\sigma_z)^2}} \right) \quad (3)$$

186 2.3.5 Gaussian Plume model parameterization

187 Data used as input to the GP model are filtered by wind direction and only air from the North
 188 Terminal (270° to 315°) in the analysis, these include: wind speed, wind direction, temperature,
 189 CH_4 mixing ratio at Rampside church, background CH_4 mixing ratio and the PGSC. The PGSC is
 190 estimated from wind speed and irradiance data (Seinfeld and Pandis, 2016), as measured by the
 191 meteorological station (Supplementary Material Section 1).

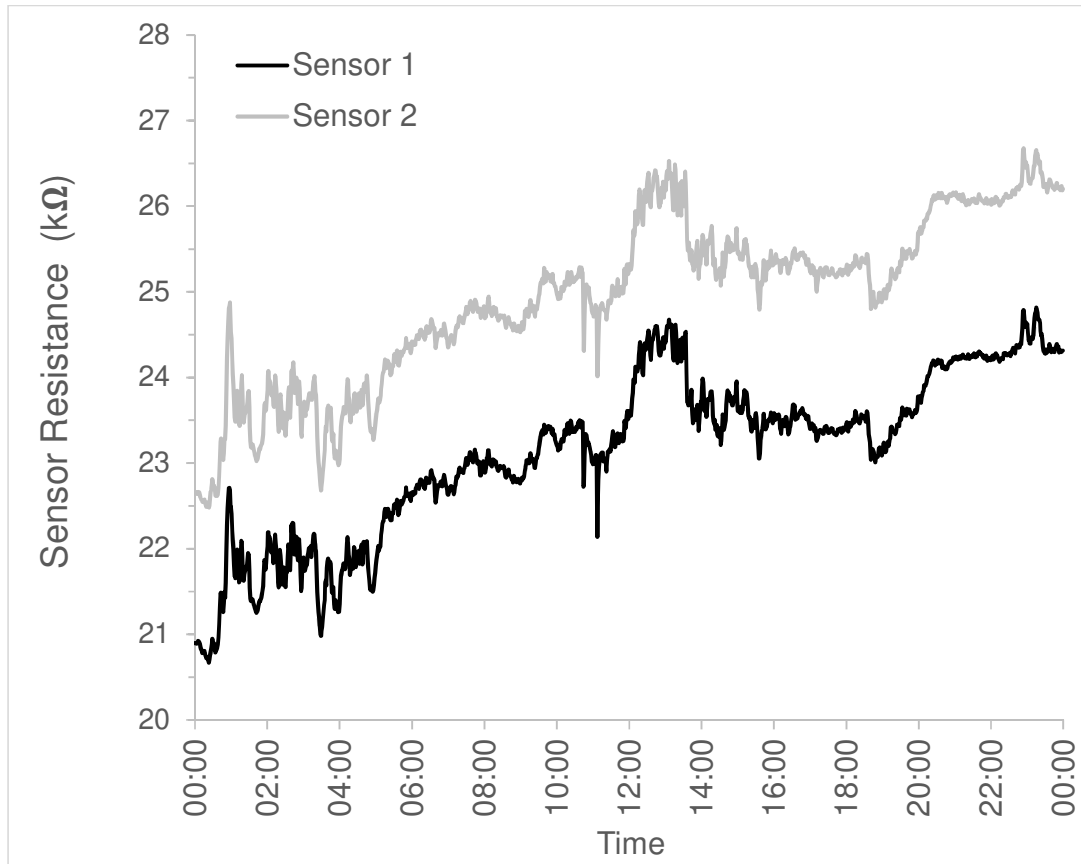
192 2.3.6 Uncertainty in emissions

193 We conducted an uncertainty analysis for the emissions using the GP approach. Scenarios were
 194 run in which individual input variables were changed and the resulting changes in average CH_4
 195 emissions calculated for the entire measurement period were tracked. Individual uncertainties were
 196 determined by the precision of the instrument: the TGS2600 (calculated below in Section 3.2); the
 197 wind speed (the result of a $\pm 0.5 \text{ m s}^{-1}$ measurement uncertainty); the air temperature ($\pm 0.5 \text{ }^\circ\text{C}$);
 198 and the uncertainty in relative humidity ($\pm 0.5 \%$). Ordinarily, we would expect there to be
 199 uncertainty in assigning a PGSC value for use in the GP model. However, we found this not to be
 200 the case here and we discuss this further in Section 3.5. An additional uncertainty is that the
 201 TGS2600 is cross-sensitive to carbon monoxide (CO), iso-butane, ethanol, and hydrogen.
 202 However, these gases are not expected to pose a significant problem of contamination at a coastal
 203 site in marine inflow conditions. An overall uncertainty for the CH_4 emission estimate is presented
 204 as the as the root mean square deviation (RMSD) of the individual uncertainties.

205 3 Results

206 3.1 TGS2600 output reproducibility

207 To test for differences in TGS2600 output between sensors from the same manufacturer, a second
 208 TGS2600 (Sensor 2, Figure 2) was run next to the original TGS 2600 sensor (Sensor 1, Figure 2)
 209 on the 3rd September 2018 at Plumpton Hall Farm, Lancashire, UK. Despite the resistance of the
 210 two sensors having nearly identical temporal response to changes in CH_4 concentrations, the
 211 resistance of the original and second sensor correlate with $R^2 = 0.995$, $m = 1.015$, $p\text{-value} = 0$,
 212 there is an offset of $1.45 \text{ k}\Omega$ between the resistance of the two sensors at the same CH_4
 213 concentration (between 1.9 and 3.3 ppm) (Figure 2).

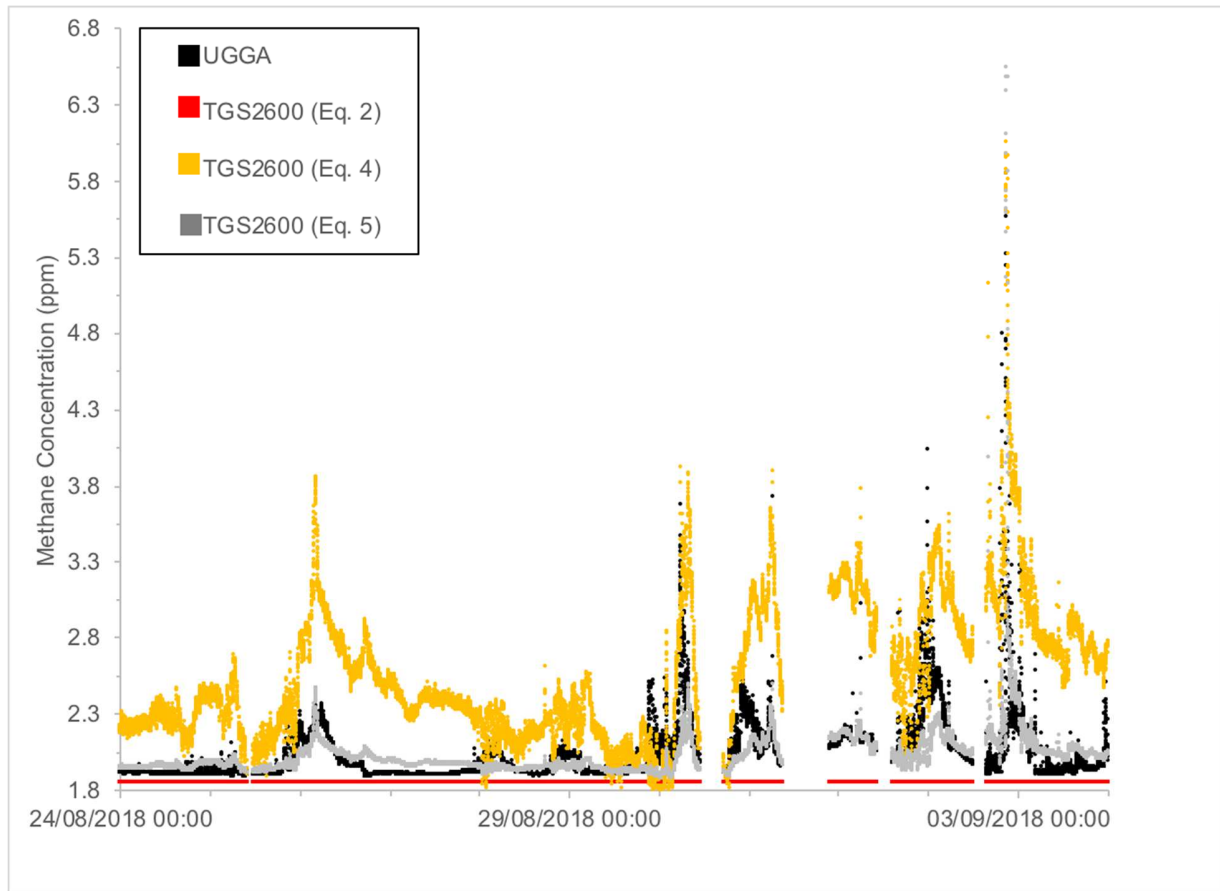


214
215
216

Figure 2 The sensor resistance from the original TGS2600 sensor (Sensor1) and a second TGS2600 (Sensor 2) run beside each other on the 3rd September 2018 at Plumpton Hall Farm, Lancashire, UK.

217 3.2 TGS2600 calibration

218 After the calibration periods of 21st April 2018, 24th June and between the 24th August 2018 and
 219 3rd September 2018, the output data of the TGS2600 were used to calculate $(R_s/R_0)_{corr}$ using Eq. 1.
 220 This $(R_s/R_0)_{corr}$ value was then used to calculate the mixing ratio $[CH_4]_{raw}$ (Eq. 2). The calculated
 221 CH_4 mixing ratios ranged from 1.85 ppm to 1.86 ppm (Red line, Figure 3) while the UGGA
 222 measurements varied between 1.85 ppm and 6.0 ppm (Black line, Figure 3). This strongly
 223 suggests that our sensor did not behave the same way as the sensor used by Eugster and Kling
 224 (2012).



225
 226 *Figure 3. Methane mixing ratios calculated by the TGS2600 output and the method of Eugster and Kling (2012) (Eq. 2; Red dots),*
 227 *TGS2600 output and a linear relationship (Eq. 4; orange dots), TGS2600 output and a non-linear relationship (Eq. 5; grey dots)*
 228 *and the UGGA (black dots) between the 24th August and 4th September 2018 at University of Manchester's Site at Plumpton Hall*
 229 *Farm.*

230 As our setup and operation were exactly the same as Eugster and Kling (2012), we suggest there
 231 could either be manufacturing differences between our TGS2600 and the sensor used by Eugster
 232 and Kling (2012) or the very narrow range of CH₄ mixing ratios measured by Eugster and Kling
 233 (2012), 1.85 to 2 ppm, means that Eq. 2 gives a poor fit at higher mixing ratios. To better calibrate
 234 the TGS2600 for a larger mixing ratio range, we calculated alternative linear and heuristically
 235 derived non-linear empirical relationships for our TGS2600 sensor using data from the UGGA to
 236 tune the algorithms (Figure 3; Table 1).

237

238 *Table 1 Comparison of algorithms to derive $[CH_4]_{raw}$ using gradient, R^2 and the area under the*
 239 *mixing ratio line in Figure 3.*

Algorithm	Eq. #	Line colour Fig. 3	Equation to calculate $[CH_4]_{raw}$	m	R^2	Area under line
UGGA		Black				34619
Eugster & Kling	2	Red	$1.8280 + 0.0288 \cdot \left(\frac{R_s}{R_0}\right)_{corr}$	0.003	0.27	31537
Linear	4	Orange	$-7.37 + 12.74 \cdot \left(\frac{R_s}{R_0}\right)_{corr}$	1.19	0.27	43833
Non-linear	5	Grey	$1.8 + 0.09 \cdot \exp\left(11.669 \cdot \left(\left(\frac{R_s}{R_0}\right)_{corr} - 0.7083\right)\right)$	0.57	0.23	34690

240

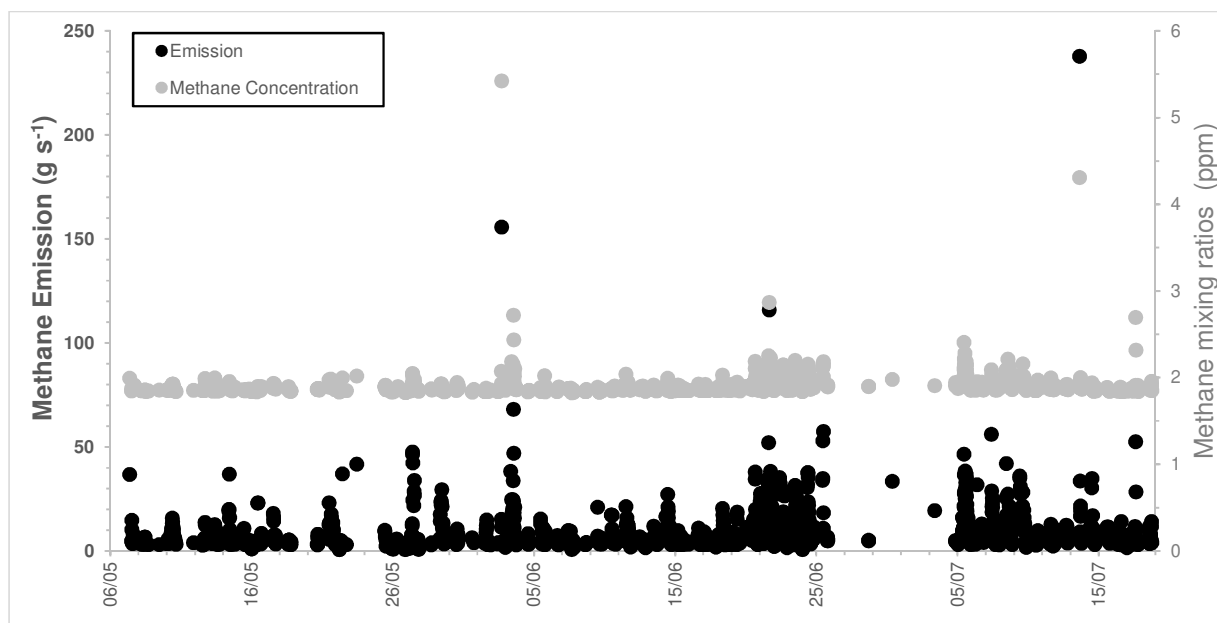
241 The gradient, m, and R^2 values of the linear regression between the $[CH_4]_{raw}$ values and the UGGA
 242 mixing values (Table 1) suggests the linear relationship (Eq. 4 Table 1; orange line Figure 3)
 243 generates the best fitting $[CH_4]_{raw}$ estimates when compared to the UGGA mixing ratios.
 244 However, when using the area under the mixing ratio curve as a metric, the non-linear algorithm
 245 (Eq. 5 Table 1; grey line Figure 3) agrees best with the area under the UGGA mixing ratios (black
 246 line Figure 3), while the linear relationship (Eq. 4 Table 1) overestimates the mass emitted by 25%.
 247 This suggests that, even though the $[CH_4]_{raw}$ mixing ratios calculated by Eq. 5 are not directly
 248 comparable, (i.e. do not occur at exactly the same time as the UGGA mixing ratios), it gives the
 249 best agreement when calculating the time averaged mixing ratio.

250 Methane mixing ratios calculated using Eq. 5 were generally slightly lower than those measured
 251 by the UGGA, with the mean difference between the TGS2600 and UGGA CH_4 mixing ratios of
 252 -0.004 ppm. Using the 95% uncertainty intervals, by comparing the UGGA CH_4 mixing ratios to
 253 those calculated from the TGS2600 output we report an uncertainty in CH_4 mixing ratios at ± 0.01
 254 ppm. The TGS2600 also took longer to respond to changes in mixing ratio than the UGGA for
 255 the range of measured mixing ratios (background concentrations of about 2 ppm to 7 ppm). We
 256 also found that over time the TGS2600 drifted by 0.002 ppm per day and the TGS2600 output was
 257 very uncertain when relative humidity was less than 40 %.

258

259 **3.3 Methane mixing ratios in air from the gas terminal**

260 Methane mixing ratios were calculated using TGS2600 measurements made at Rampside church
 261 and calculated using Eq. 5. These calculated CH_4 mixing ratios indicate enhancements can be
 262 observed most of the time when the wind comes from the North Terminal (Figure 4). The largest
 263 enhancement, 5.4 ppm, was observed on the 2nd June 2018 (grey dots; Figure 4) with the mean CH_4
 264 mixing ratio of 2.0 ppm detected over the three months. The background mixing ratio was taken as
 265 the minimum mixing ratio over a rolling 24 hour period to capture intermittent enhancements from
 266 other sources in the “background” measurement.



267
 268 *Figure 4 Time series of 15-minute averaged CH₄ concentrations measured by the TGS2600 at St Michael's Church and calculated*
 269 *CH₄ emissions using Eq. 5 from Rampside gas terminal, Rampside, Cumbria.*

270 **3.4 Methane emissions from the gas terminal**

271 Fifteen-minute averaged CH₄ emissions from the Rampside gas terminal were calculated with the
 272 Gaussian plume model using measured mixing ratios and matching meteorological data (as
 273 described in Section 3.3). As the location of emissions within each terminal is unknown, for the
 274 purpose of this calculation we assume the mixing ratio measured by the sensor corresponds to the
 275 centre of a Gaussian plume (i.e. the peak value) whenever the wind direction is between 270° and
 276 315° for the North Terminal and between 225° and 270° for the South Terminal. For other wind
 277 directions no emission rate is calculated for either terminal.

278 Under this assumption we calculate a maximum emission from the North Terminal of 238 g s⁻¹,
 279 observed on the 13th July (black dots; Figure 4), with a mean emission from the North Terminal of
 280 9.6 g s⁻¹. This is over six times higher than the mean emission of 1.6 g s⁻¹ calculated for the South
 281 Terminal during the same period. Our results suggest that even though gas is not passing through
 282 the South Terminal, residual CH₄ continues to be emitted from the site.

283 Assuming the measured mixing ratio in air that has passed over either terminal is representative of
 284 the centre of a Gaussian plume is clearly a significant simplification. Emissions within each
 285 terminal are likely to emanate from one or several point sources. Therefore, our calculated mean
 286 emission rate will be biased low, as in reality many of our measurements will not represent the
 287 central (maximum) mixing ratio within the plume. Using only a single sensor we do not have
 288 enough information to constrain both spatial and temporal emission patterns. We present the
 289 emission estimates above to demonstrate the potential utility of these sensors; they are not intended
 290 to be considered as accurate estimates of typical emissions from this site on annual timescales.

291 **3.5 Uncertainty in emission estimates**

292 As discussed in Section 2.3.6, we would expect there to be uncertainty in assigning a PGSC when
 293 using a GP model. Here we have found little uncertainty at the site as it was very windy and the

294 wind from the gas terminal to the church was from the open ocean. This meant that for 75% of
295 the measurements the wind was greater than 6 m s^{-1} , i.e. corresponding to neutral conditions
296 (Supplementary Materials Section 1), with the remaining 25% in slightly unstable conditions.

297 We estimate that contamination by CO, iso-butane, ethanol, and hydrogen will not affect the
298 TGS2600 CH₄ mixing ratio measurements, assuming the gas terminal is not the source of the
299 contamination. Any background increase in contaminant mixing ratio will result in an increase in
300 the rolling background mixing ratio which will be included when calculating the CH₄ emission
301 using the GP model.

302 Scenarios were run using the GP model to reflect variability in the TGS2600 measured CH₄ mixing
303 ratio ($\pm 0.01 \text{ ppm}$), air temperature, wind speed and relative humidity. Uncertainties in air
304 temperature ($\pm 0.5 \text{ }^\circ\text{C}$) affected the calculated average emission the most ($\pm 13 \%$). This was
305 similar to the uncertainties in wind speed ($\pm 9 \%$) and TGS2600 CH₄ mixing ratio ($\pm 8 \%$), while
306 the uncertainty in relative humidity ($\pm 0.5 \%$) affected the average calculated emission the least (\pm
307 3%). We estimate the RMSD in average CH₄ emission calculated over the measurement period
308 to be $\pm 18 \%$.

309 **4 Discussion**

310 **4.1 Low-cost sensor**

311 Our direct comparison of the CH₄ mixing ratios measured by the TGS2600 and the UGGA indicate
312 that the TGS2600 can be used to reliably measure CH₄ mixing ratios from 1.8 up to 6 ppm using
313 an empirical correction. The main drawback to the TGS2600 is that the sensor output representing
314 low CH₄ mixing ratios (between 1 to 10 ppm) appears to be highly variable between sensors.
315 However, since only two sensors were tested, we cannot yet assess the typical variability for a
316 larger number of sensors. The differences between individual sensors may be due to differences in
317 manufacturing that affect R_s at low CH₄ mixing ratios, and requires a high-precision instrument to
318 calibrate the sensor. The algorithm Eugster and Kling (2012) used to calculate CH₄ mixing ratios
319 (Eq.2) was different from the non-linear empirical relationship used in this study (Eq. 5) and may
320 reflect significant differences in individual sensor response to changes in CH₄ concentrations. This
321 means that the TGS2600 may only be useful to those with access to high-precision CH₄
322 instruments. We suggest manufacturers could make these simple sensors more consistently if they
323 were looking to market the TGS2600 as an accurate “off the shelf” CH₄ sensor. Without this, we
324 conclude that empirical corrections may need to be derived for individual sensors to yield
325 meaningful data.

326 In addition to the calibration, the TGS2600 did not to respond to changes in mixing ratio exactly
327 at the same time as the UGGA. This is expected to be related to the passive nature of the TGS2600
328 sensor in contrast to the UGGA, where air is pumped through the measurement cavity. The
329 TGS2600 sensor cannot be calibrated using calibration gases as the very low humidity of these
330 gases (<40%) result in unstable output. The most accurate method for calibration was found to
331 be running the TGS2600 next to a high-precision instrument for a period of time. The TGS2600
332 was also noted to drift over time. Our measurements estimate the output varied by 0.002 ppm per
333 day indicating that calibration checks should be made frequently to ensure that any drift is
334 corrected and remains linear over time. We suggest that, for a sensor with similar output to the
335 one used in the study, calibrations every two months should be adequate to quantify any drift, i.e.
336 the drift over two months of 0.12 ppm should be observable.

337 Aside from these negatives, the TGS2600 succeeded in measuring CH₄ mixing ratios, within ±
338 0.01 ppm to mixing ratios measured by the UGGA, autonomously and continuously over a period
339 of three months. The power consumption meant that it could be run for seven days from a 35 Ah
340 lead acid battery. The TGS2600 output was logged to an SD card, the CH₄ mixing ratio calculated
341 by post-processing, and the CH₄ emissions from a source calculated using a Gaussian Plume
342 model. These data confirm the proof of concept that individual TGS2600 sensors could be run as
343 part of a network to estimate changes in the CH₄ emission landscape, however their measurements
344 are only inter-comparable and reliable if they are frequently calibrated with an high precision
345 instrument.

346 **4.2. Methane emissions from the Rampside Gas terminal**

347 The measurements made at St Michael's Church, Rampside, 1.5 km from the source, estimated
348 the average CH₄ emission from the Rampside gas North Terminal between May and August 2018
349 at 9.6 g CH₄ s⁻¹ with a peak emission of 238 g CH₄ s⁻¹. In addition, we measured an average CH₄
350 emission from the decommissioned South Terminal of 1.6 g s⁻¹. The identification of non-zero
351 emissions from the South Terminal demonstrates the utility of direct emission monitoring using
352 continuous ground-based measurement. To give these emissions some context, the average
353 emission from the North Terminal can be used to extrapolate up to an annual estimate of 0.30 Gg
354 CH₄ yr⁻¹, which is comparable to the 2018 UK National Atmospheric Emissions Inventory (NAEI)
355 emission estimate of 0.45 Gg CH₄ yr⁻¹. The difference between our estimate and the NAEI estimate
356 is expected as the single sensor method and simple Gaussian analysis used in this study was
357 predicted to underestimate the emission.

358 Overall, this study shows that a low-cost sensor can be used to make direct CH₄ mixing ratio
359 measurements and the data collected can be used to calculate realistic CH₄ emissions from an
360 onshore gas terminal. In contrast to emission factor generated values, which only estimate
361 emission from known sources, direct measurements can show temporal and geographical
362 variability in emissions and can be used to indicate where and when unknown leakage of CH₄
363 occurs. Many sensors surrounding the perimeter of the site networked together could be used to
364 explicitly identify the size and location any source of leakage in almost real-time and the problem
365 could be fixed before significant CH₄ is lost to the atmosphere.

366 **4.3 Implications for large low-cost sampling networks for methane**

367 Although some additional uncertainty in emission estimates may be unavoidable when low-cost
368 sensors are used, this study indicates that low-cost sensors, when properly calibrated against high-
369 precision instruments, can overcome many of the logistical and cost issues associated with higher-
370 cost, high-precision sensors and can be used to monitor emissions locally and at a distance from
371 a source. We suggest that networks of low-cost sensors could be deployed and provide a “first-
372 look” at local emission landscapes over a wider area and longer time period than is possible with
373 costly sensors and can be used to identify emission hot-spots that should be investigated further
374 using high-precision instruments. Such a wide deployment of low-cost sensors would facilitate
375 more realistic greenhouse gas inventories than those currently developed using emission factors
376 and activity levels that do not fully capture the actual leakage processes that may be occurring.

377 **Author contributions**

378 S. N. Riddick and D. L. Mauzerall designed the experiment. S. N. Riddick, J. C. Riddick, G. Allen
379 and J. Pitt prepared equipment, calibrated the instruments, carried out the measurements and

380 provided analysis. D. L. Mauzerall and M. Celia were the project leaders and provided scientific
381 oversight and guidance throughout the planning, implementation, collection, and data analysis
382 processes. S. N. Riddick and D. L. Mauzerall wrote the paper with help from M. Celia and M.
383 Kang and with contributions from all co-authors.

384 **Acknowledgements**

385 We would like to thank the curators of St Michaels Church, Rampside, Jim and Brenda Webster
386 for their assistance during the measurement campaign as well as the Reverend Lucie Lunn for
387 allowing us to measure at the church. We also acknowledge funding from the National Oceanic
388 and Atmospheric Administration (Grant # AWD1004141) and Princeton University's Science,
389 Technology, and Environmental Policy (STEP) program for research support.

390 **References**

- 391
392 BEIS, 2018. UK greenhouse gas emissions statistics [WWW Document]. GOV.UK. URL
393 <https://www.gov.uk/government/collections/uk-greenhouse-gas-emissions-statistics>
394 (accessed 11.26.18).
395 Busse, A.D., Zimmerman, J.R., 1973. User's Guide for the Climatological Dispersion Model.
396 National Environmental Research Center, Office of Research and Development, U.S.
397 Environmental Protection Agency.
398 Cerri, C.E.P., You, X., Cherubin, M.R., Moreira, C.S., Raucci, G.S., Castigioni, B. de A., Alves,
399 P.A., Cerri, D.G.P., Mello, F.F. de C., Cerri, C.C., 2017. Assessing the greenhouse gas
400 emissions of Brazilian soybean biodiesel production. PLOS ONE 12, e0176948.
401 <https://doi.org/10.1371/journal.pone.0176948>
402 de Coninck, H., Revi, A., Babiker, M., Bertoldi, P., Buckeridge, M., Cartwright, A., Dong, W.,
403 Ford, J., Fuss, S., Hourcade, J. C., Ley, D., Mechler, R., Newman, P., Revokatova, A.,
404 Schultz, S., Steg, L. and Sugiyama, T., 2018. Global warming of 1.5°C: Summary for
405 policy makers. IPCC - The Intergovernmental Panel on Climate Change , p. 313-443 131
406 p.
407 Connors, S., Manning, A.J., Robinson, A.D., Riddick, S.N., Forster, G.L., Ganesan, A., Grant,
408 A., Humphrey, S., O'Doherty, S., Oram, D.E., Palmer, P.I., Skelton, R.L., Stanley, K.,
409 Stavert, A., Young, D., Harris, N.R.P., 2018. Estimates of sub-national methane
410 emissions from inversion modelling. Atmospheric Chem. Phys. Discuss. 1–19.
411 <https://doi.org/10.5194/acp-2018-1187>
412 DEFRA, 2019. UK National Atmospheric Emissions Inventory (NAEI) Data - Defra, UK
413 [WWW Document]. URL <http://naei.beis.gov.uk/data/> (accessed 8.12.19).
414 Eugster, W., Kling, G.W., 2012. Performance of a low-cost methane sensor for ambient
415 concentration measurements in preliminary studies. Atmospheric Meas. Tech. 5, 1925–
416 1934. <https://doi.org/10.5194/amt-5-1925-2012>
417 Figaro, 2005. TGS 2600 – for the detection of air contaminants, On- line product data sheet,
418 <http://www.figarosensor.com/products/2600pdf.pdf> [WWW Document]. URL
419 <http://www.figarosensor.com/products/2600pdf.pdf> (accessed 2.25.19).
420 IPCC, 2018. Summary for Policymakers — Global Warming of 1.5 °C. URL
421 <https://www.ipcc.ch/sr15/chapter/summary-for-policy-makers/> (accessed 12.18.18).
422 NOAA, 2019. ESRL Global Monitoring Division - Global Greenhouse Gas Reference Network
423 [WWW Document]. URL https://www.esrl.noaa.gov/gmd/ccgg/trends_ch4/ (accessed
424 6.14.19).

425 OGA, 2018. UK Oil and Gas Authority [WWW Document]. URL [https://data-](https://data-ogauthority.opendata.arcgis.com/pages/production)
426 [ogauthority.opendata.arcgis.com/pages/production](https://data-ogauthority.opendata.arcgis.com/pages/production) (accessed 11.27.18).

427 Pasquill, F., 1975. Limitations and Prospects in the Estimation of Dispersion of Pollution on a
428 Regional Scale, in: *Advances in Geophysics*. Elsevier, pp. 1–13.
429 [https://doi.org/10.1016/S0065-2687\(08\)60568-3](https://doi.org/10.1016/S0065-2687(08)60568-3)

430 Riddick, S.N., Connors, S., Robinson, A.D., Manning, A.J., Jones, P.S.D., Lowry, D., Nisbet, E.,
431 Skelton, R.L., Allen, G., Pitt, J., Harris, N.R.P., 2017. Estimating the size of a methane
432 emission point source at different scales: from local to landscape. *Atmospheric Chem.*
433 *Phys.* 17, 7839–7851. <https://doi.org/10.5194/acp-17-7839-2017>

434 Riddick, S.N., Hancock, B.R., Robinson, A.D., Connors, S., Davies, S., Allen, G., Pitt, J., Harris,
435 N.R.P., 2018. Development of a low-maintenance measurement approach to continuously
436 estimate methane emissions: A case study. *Waste Manag.* 73, 210–219.
437 <https://doi.org/10.1016/j.wasman.2016.12.006>

438 Riddick, S.N., Mauzerall, D.L., Celia, M., Harris, N.R.P., Allen, G., Pitt, J., Staunton-Sykes, J.,
439 Forster, G.L., Kang, M., Lowry, D., Nisbet, E.G., Manning, A.J., 2019a. Methane
440 emissions from oil and gas platforms in the North Sea. *Atmospheric Chem. Phys.* 19,
441 9787–9796. <https://doi.org/10.5194/acp-19-9787-2019>

442 Riddick, S.N., Mauzerall, D.L., Celia, M.A., Kang, M., Bressler, K., Chu, C., Gum, C.D., 2019b.
443 Measuring methane emissions from abandoned and active oil and gas wells in West
444 Virginia. *Sci. Total Environ.* 651, 1849–1856.
445 <https://doi.org/10.1016/j.scitotenv.2018.10.082>

446 Seinfeld, J.H., Pandis, S.N., 2016. *Atmospheric chemistry and physics: from air pollution to*
447 *climate change*, Third edition. ed. John Wiley & Sons, Inc, Hoboken, New Jersey.

448 Turner, D.A., Williams, I.D., Kemp, S., 2015. Greenhouse gas emission factors for recycling of
449 source-segregated waste materials. *Resour. Conserv. Recycl.* 105, 186–197.
450 <https://doi.org/10.1016/j.resconrec.2015.10.026>

451 US EPA, 1995. *Industrial Source Complex (ISC3) Dispersion Model*, Research Triangle Park,
452 NC: U.S. Environmental Protection Agency. User’s Guide. EPA 454/B 95 003a (vol. I)
453 and EPA 454/B 95 003b (vol. II).

454 Yang, W.-B., Yuan, C.-S., Chen, W.-H., Yang, Y.-H., Hung, C.-H., 2017. Diurnal Variation of
455 Greenhouse Gas Emission from Petrochemical Wastewater Treatment Processes Using
456 In-situ Continuous Monitoring System and the Associated Effect on Emission Factor
457 Estimation. *Aerosol Air Qual. Res.* 17, 2608–2623.
458 <https://doi.org/10.4209/aaqr.2017.08.0276>
459
460

461 Supplementary Material Section 1

462

463 Estimating the stability class from wind speed and sunlight conditions (Pasquill, 1974).

464

Stability Class	Day			Night		
	Wind Speed (m s ⁻¹)	Strong	Mod	Light	Overcast	Clear
2		a	a	b		
3		b	b	c	e	f
4		b	c	c	d	e
5		c	c	d	d	d
6		c	d	d	d	d

465

466